

AMERICAN UNIVERSITY OF BEIRUT

VENTILATION BENEFITS WHEN USING RADIATIVE
COOLING COMBINED WITH PHASE CHANGE
MATERIALS (PCM) STORAGE IN HOT CLIMATES

by
JENNYFER SASSINE KARAM

A thesis
submitted in partial fulfillment of the requirements
for the degree of Master of Engineering
to the Department of Mechanical Engineering
of the Maroun Semaan Faculty of Engineering and Architecture
at the American University of Beirut


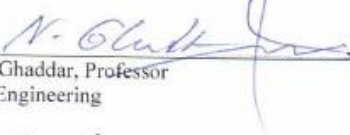

Beirut, Lebanon
August, 2021

AMERICAN UNIVERSITY OF BEIRUT

VENTILATION BENEFITS WHEN USING RADIATIVE COOLING
COMBINED WITH PHASE CHANGE MATERIALS (PCM)
STORAGE IN HOT CLIMATES

by
JENNYFER SASSINE KARAM

Approved by:

 _____	_____
Dr. Kamel Abou Ghali, Professor Mechanical Engineering	Advisor
 _____	_____
Dr. Nesreen Ghaddar, Professor Mechanical Engineering	Co-Advisor
 _____	_____
Dr. Fadl Moukalled, Professor Mechanical Engineering	Member of Committee

Date of thesis defense: August 24, 2021

ACKNOWLEDGEMENTS

The authors would like to acknowledge the Kuwait Foundation for the Advancement of Sciences (KFAS) for supporting this research grant number: AP1835EM01.

ABSTRACT OF THE THESIS OF

Jennyfer Sassine Karam

for

Master of Engineering

Major: Mechanical Engineering

Title: Ventilation benefits when using radiative cooling combined with phase change materials (PCM) in hot climates

In this work, a passive system composed of a radiative cooling (RC) panel combined with two phase change material (PCM) storage tanks was integrated with the conventional air conditioning (AC) system to offset the increase in energy consumption related to the conditioning of the high temperature fresh air intake in the hot climate of Kuwait. The cooling power produced by the RC panel was used to charge the PCM storage tanks. One of these tanks was used for precooling the supplied fresh air and another for enhancing the coefficient of performance (COP) of the AC system by cooling the ambient air entering the condenser. A mathematical model was developed for the proposed system and a set of simulations was conducted for a typical Kuwaiti residence for the entire summer season extending from April to October.

It was found that using tank 1 to precool the fresh air supplied to the space resulted in an increase in the fresh air intake at zero energy expenses: no ventilation load was required from the AC system. Furthermore, the use of tank 2 has led to an enhancement of 10.5 % of the COP. Thus, the overall energy consumption of the AC system was reduced by 22.3 % with respect to the conventional AC system.

TABLE OF CONTENTS

ACKNOWLEDGEMENTS	1
ABSTRACT	2
ILLUSTRATIONS	5
TABLES	6
ABBREVIATIONS	7
INTRODUCTION	8
SYSTEM DESCRIPTION	12
A. Daytime system operation.....	13
B. Early night system operation.....	14
C. Late night system operation	14
MATHEMATICAL MODELING	17
A. Hydronic radiative cooling panel.....	17
B. PCM tanks model.....	18
C. The Space Model.....	21

NUMERICAL METHODOLOGY	22
CASE STUDY	26
RESULTS	30
A. Model validation	30
B. System sizing	31
C. System operation	33
D. Energy saving analysis	38
CONCLUSION	40
REFERENCES	41

ILLUSTRATIONS

Figure

1.	Schematic of the complete hybrid system and its daytime operation.....	13
2.	Schematic of: (a) Early night operation of the system and (b) late night operation of the system.....	15
3.	Schematic of the RC panel discretized into segments and different heat transfer processes.....	18
4.	Schematic of one PCM tank during solidification (nighttime) and melting (daytime).....	19
5.	Flow chart of the numerical modeling methodology.....	23
6.	Hourly variation of temperature and solar radiation for a representative day of each cooling month.....	28
7.	Flow rate of fresh air supplied to the space for the entire cooling season.....	34
8.	Average ventilation savings for a representative day of the cooling season..	36
9.	Average additional savings in the cooling load for a representative day of the cooling season.....	36
10.	Hourly schedule of the PCM tank 2 operation and corresponding percentage of COP enhancement for each considered summer month.....	37
11.	Average percentage reduction of the energy consumption using the proposed system with respect to the conventional mechanical cooling system for the entire summer season.....	39

TABLES

Table

1.	Thermal details of the envelope layers (Inside to Outside)	29
2.	Characteristics of the PCM storage tanks.....	33

ABBREVIATIONS

A	Area (m ²)
C_p	Specific heat (kJ/kg.K)
dt	Time step (s)
f	Melted fraction
h	Convective heat coefficient (W/m ² .K)
\dot{m}	Mass flow rate (kg/s)
N_{pcm}	Number of PCM spheres in each tank segment
PCM	Phase change materials
RC	Radiative cooling
T	Temperature (°C)
$Tm1$	Melting temperature of PCM tank 1
$Tm2$	Melting temperature of PCM tank 2
V	Volume (m ³)
Subscripts	
W	Water
1	Tank 1
2	Tank 2

CHAPTER I

INTRODUCTION

During the last decades, the need for cooling in the building sector has witnessed a dramatic increase due to population growth, urbanization and climate change. This is especially true for countries in the Gulf region usually characterized by hot summers [1]. Moreover, the need for an immaculate quality of the inhaled air indoors has become a necessity in the era of the covid-19 pandemic spread in tight conditioned building, and the need to increase fresh air ventilation to dilute biological indoor contaminants and reduce cross-contamination between occupants [2, 3].

Both the domestic and non-residential building stock in the Gulf region rely heavily on mechanical cooling and ventilation installations [4, 5] However, such techniques are expensive, energy-intensive, and can further exacerbate the climate change problem by contributing to greenhouse gases emissions [6]. In contrast with conventional air conditioning, passive cooling techniques – given adequate design and control of supply conditions, can provide the same cooling effect with limited environmental impacts and allow the increase in the ventilation loads; hence improve indoor air quality (IAQ) at reduced energy costs.

Many passive and cost-effective cooling strategies have been extensively studied in the literature. Some of these strategies rely on smart employment of the building fabric (i.e., louver shading devices, double glazed windows, insulation, reflective paints...) [7, 8] or on the passive cooling of the supply air through water evaporation (direct, indirect evaporative cooling) [9, 10]. Another emerging technique is the use of radiant cooling, which takes places through the net emission of electromagnetic waves

from warm objects to cool ones. The setup consists of a specialized metallic plate that emits long-wave radiation to the outer space (i.e., heat sink) for cooling purposes. The emitted radiation escapes through the transparency window of the atmosphere (8-13 μm) in which the radiative emission exceeds the incoming absorbed radiation from the sun. This phenomenon is outweighed by the absorbed solar and atmospheric radiation outside the transparency window. Many studies considered enhancing the conventional radiative cooling (RC) panels [11-15] through the use of new coating materials that are spectrally selective, having a high emissivity inside the atmospheric transparency window and low absorptivity outside it [11-13]. In addition, such materials also have high solar reflectivity in order to avoid the absorption of incident solar radiation by the RC panel during daytime [14, 15].

Despite all the efforts to increase its effectiveness, RC faces many challenges in building applications especially in hot climate countries [16]. First, the RC power is not enough for large building cooling demands [17]. Consequently, it is considered as an assistive system to the conventional air conditioning system. Jeong et al. [18] suggested that the passive RC system should be integrated with a conventional air conditioning system to precool the fresh hot air supplied to the space. They found that the proposed system was able to achieve 35% potential saving in energy consumption. Second, the cooling power of RC panels varies vastly between nighttime and daytime. In the absence of shortwave radiation, the highest cooling power of the RC panels occurs at night while building occupants require more cooling in the daytime [17, 19]. Bao et al. [20] theoretically showed that under dry air conditions coated panels can achieve about 17 °C below ambient at night and 5 °C below ambient under direct solar radiation. To alleviate this problem many literature studies implemented storage systems with RC

applications to store the RC cooling energy and use it during peak cooling demand hours [21, 22].

Phase change materials (PCM) used in thermal storage tanks have gained a lot of attention especially when combined with RC system. These materials have the capability to store thermal energy at relatively constant temperature (i.e., melting temperature) due to their high heat capacity and reduce system energy consumption. PCM is available in wide melting temperature range. A proper storage temperature is an important criterion for selection of a suitable PCM for passive applications [22, 23]. The PCM melting temperature is selected in such a way to enable complete solidification process during nighttime and complete melting process during daytime [24]. As the cooling power of the RC panel is low during daytime and increases throughout the night [25], this work suggests the use of two PCM storage tanks at two different melting temperatures to ensure total harvesting of nighttime cooling power. Thereafter, the RC cooling power, is stored at two different temperatures, to be used according to the cooling and ventilation needs in the building. On one hand, the low temperature PCM tank can make it possible to meet the entire ventilation load at increased fresh air intake, thereby passively enhancing the IAQ. On the other hand, the high temperature PCM tank can be used to lower the temperature of the air cooling the condenser of the vapor compression system in order to increase its coefficient of performance (COP) during peak hours of the day.

In this work, the implementation of RC system with two PCM storage tanks is investigated to assess the system impact on reducing the cooling loads of a residential space while passively increasing the IAQ through a case study of a typical residence in dry-hot climate of Kuwait. The study is performed for the cooling months of Kuwait

extending from April until October. The system consists of a hydronic RC panel combined with two PCM storage tanks at two different melting temperatures for day and nighttime ventilation purposes as well as an enhanced mechanical system operation resulting in a decrease in the overall energy consumption. An integrated mathematical model of the proposed system is developed to investigate the advantages of the proposed system in passively increasing the amount of fresh air supplied to the space throughout the day. In addition, the model studies the enhancement in the performance of the air conditioning system during peak hours of the day by precooling the air entering the condenser of the air conditioning unit.

CHAPTER II

SYSTEM DESCRIPTION

A hybrid cooling system composed of the conventional vapor compression AC system and a RC-PCM system is considered in this work to meet the ventilation needs of a typical Kuwaiti villa, and reduce the AC system's energy consumption by enhancing its performance. The RC-PCM system assists the vapor compression AC system in meeting the entire ventilation load while increasing the fresh airflow supplied ($\dot{m}_{fresh\ air}$) to the villa, at zero energy cost compared to the standalone mechanical cooling system. Furthermore, the performance of the AC system is enhanced by increasing its COP and reducing the overall required cooling load. The RC-PCM system consists of a hydronic RC panel with two PCM thermal storage tanks at two different melting temperatures:

- PCM tank 1 at low melting temperature ($Tm1$): it is used for precooling the fresh air to meet the ventilation load;
- PCM tank 2 at high melting temperature ($Tm2$): it is used to improve the efficiency of the vapor compression system by increasing its coefficient of performance (COP) during peak day hours.

The complete system is shown in Figure 1. The system operation varies between three time periods based on weather conditions: a) daytime operation (Figure 1), b) early night operation (Figure 2.a), and c) late night operation (Figure 2.b). Each mode of operation is described in detail in this section.

A. Daytime system operation

During daytime (Figure 1), the fresh air is cooled via an air-water heat exchanger (HE 1) with the cold water exiting the RC panel. The water leaving, HE 1 is circulated back to the RC panel to be cooled again in a closed loop. The cooled fresh air flows then to a second heat exchanger (HE 2) where it releases its heat to the exhaust air leaving the space. This is referred to as the “heat recovery” stage. The cooled air then flows into a third heat exchanger (HE 3) for cooling via heat exchange with the water exiting PCM tank 1. The exhaust water is circulated back to tank 1 in a closed loop where it loses its heat to the PCM. The exhaust air enters the mixing unit where it is mixed with the return air for further cooling in the AC system to meet the space cooling load. As for the cold energy stored in PCM tank 2, it is used to precool the air entering the condenser of the AC system to enhance its COP at peak hours, when the outdoor air temperature is higher than the PCM tank 2 melting temperature (T_{m2}) and the COP is at its lowest.

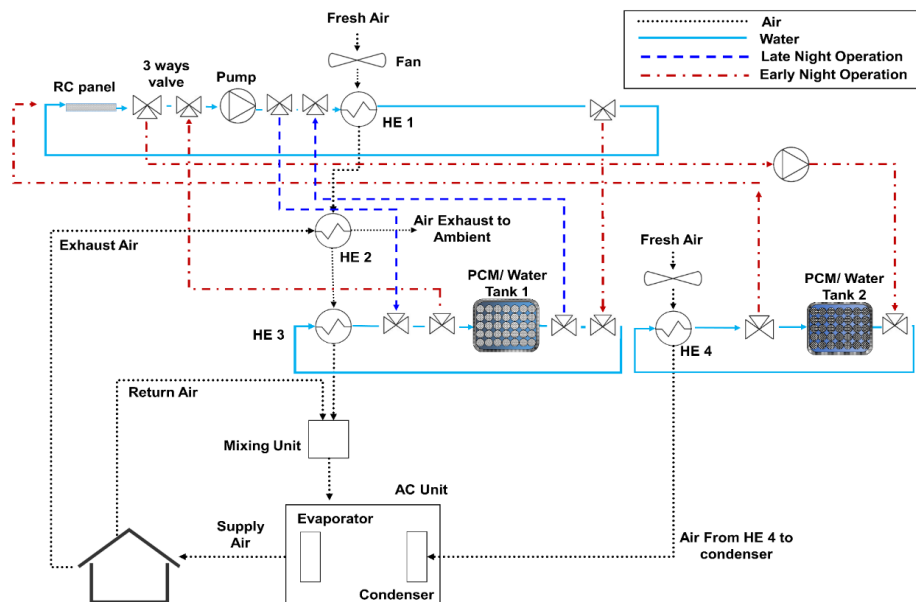


Figure 1. Schematic of the complete hybrid system and its daytime operation.

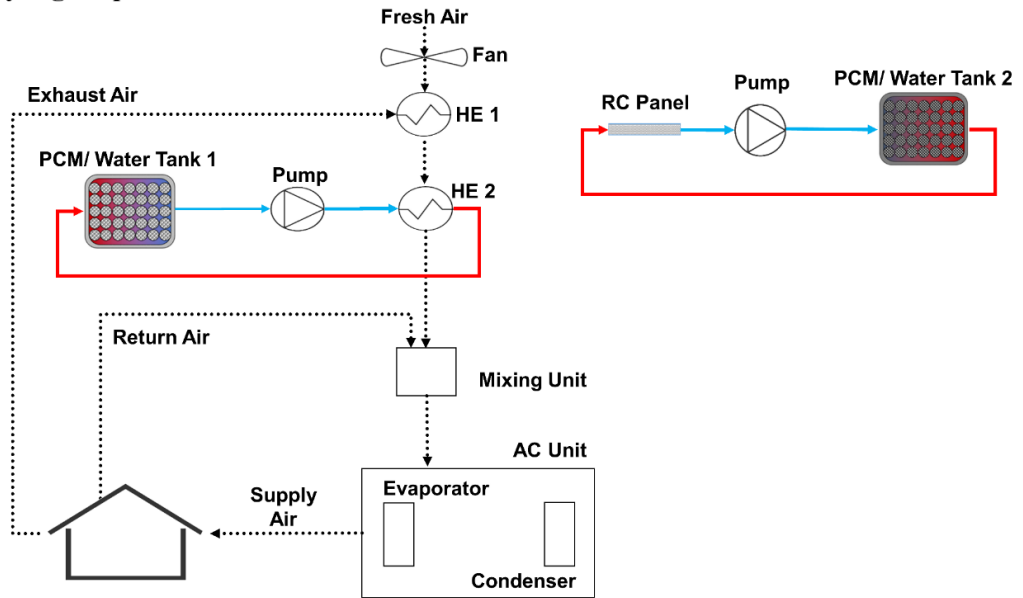
B. Early night system operation

During early hours of the night (Figure 2.a), when the temperature of the water exiting the RC panel is higher than the melting temperature of PCM tank 1 (T_{m1}), the early night operation is on. During this period, the cooling power of the RC panel is used to solidify PCM tank 2. At the same time, the fresh air is being cooled by heat recovery process via an air-air heat exchanger (HE 1) with the exhaust air. The fresh air then flows into a second heat exchanger (HE 2) where it is further cooled by the water exiting PCM tank 1. The water is circulated back to tank 1 in a closed loop where it loses its heat to the PCM. The cooled fresh air leaving HE 2 enters a mixing unit where it is mixed with the return air from the space. The product air is then supplied to the AC unit for further cooling.

C. Late night system operation

During late hours of the night (Figure 2.b), when the cooling power of the RC panel increases, the water temperature leaving the hydronic panel reaches levels below T_{m1} . Thus, this cooling power is harvested in solidifying PCM tank 1. PCM tank 2 would be completely solidified by this time due to its proper sizing. The cold-water out of the RC panels flows to PCM tank 1 where the low temperature cold energy is stored at T_{m1} . The fresh air that is first cooled by heat recovery process in HE 1, then enters an air-water heat exchanger (HE 2) where it is further cooled by the water out of PCM tank 1. The water then returns into the RC panel, whereas the fresh air undergoes the mixing process with the return air. Afterwards, air is supplied to the AC unit to meet the required cooling load of the space.

a) Early night operation



b) Late night operation

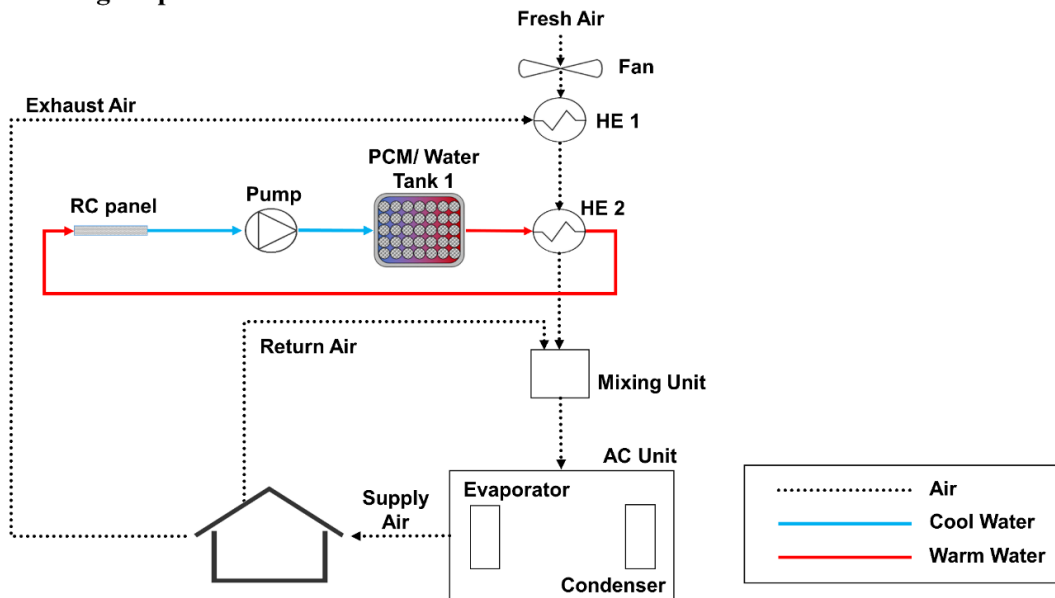


Figure 2: Schematic of: (a) Early night operation of the system and (b) late night operation of the system.

The aim of the proposed system is to increase $\dot{m}_{fresh\ air}$ supplied to the space, by harvesting the cooling power of PCM tank 1. Note that the amount of increase depends on many factors such as the size of the PCM storage tank and RC panel, as well as the outdoor conditions. The obtained increase in fresh air helps in improving the air quality indoors without any additional energy consumption. Furthermore, using PCM tank 2, the COP of the AC is enhanced by the pre-cooling of the air entering the condenser. This is expected to reduce the total energy consumption of the system with respect to the conventional AC providing the same indoor air quality (i.e. same amount of fresh air $\dot{m}_{fresh\ air}$).

CHAPTER III

MATHEMATICAL MODELING

In this section, simplified energy balance equations were derived for each component of the proposed system: the hydronic RC panel and the two PCM storage tanks. These models were adopted from Katramiz et al. [22] and integrated to simulate the operation of the system and predict the ability of the proposed system in reducing the energy consumption of the AC system.

A. Hydronic radiative cooling panel

The model of the RC panel was used to predict the water temperature through the pipes of the RC panel (Figure 3). It assumes a unidirectional variation of the water temperature through the pipes of the RC. Consequently, the panel is discretized into different segments along its length as shown in Figure 3, each having the same area A_k , and is characterized by a uniform surface temperature and a constant water temperature $T_{w,RC}$. Equation (1) presents the energy balance on a segment k :

$$\rho_w V_k C_{p,w} \frac{dT_{w,RC}(t, k)}{dt} = \dot{m}_{w,RC} C_{p,w} (T_{w,RC}(t, k-1) - T_{w,RC}(t, k)) - Q_{net} A_k \quad (1)$$

The left term of equation (1) represents the transient storage term. The first term to the right is the net convective heat flow and the last term is the time dependent net cooling power term. V_k is the volume of water in segment k . ρ_w and $C_{p,w}$ are the density and the specific heat capacity of the water, respectively. $T_{w,RC}(t, k-1)$ and $T_{w,RC}(t, k)$ are respectively the inlet and outlet water temperature of segment k at time t . $\dot{m}_{w,RC}$ is the

mass flow rate of water through the pipes embedded in the RC panel. $Q_{net}(t, k)$ is the time dependent net cooling power per unit area of segment k of the RC; it depends on several heat transfer processes as shown in Figure 3, and is described by the energy balance in equation (2):

$$Q_{net}(t, k) = Q_{rad}(t, k) - Q_{atm}(t) - Q_{sun}(t) - Q_c(t, k) \quad (2)$$

Where Q_{rad} is the longwave radiative power emitted by the panel surface, Q_{atm} is the absorbed incident atmospheric radiation, Q_{sun} is the absorbed incident solar radiation, and Q_c is the power lost/gained by the RC panel due to heat exchange via convection with the ambient air as well as conduction through the insulated roof.

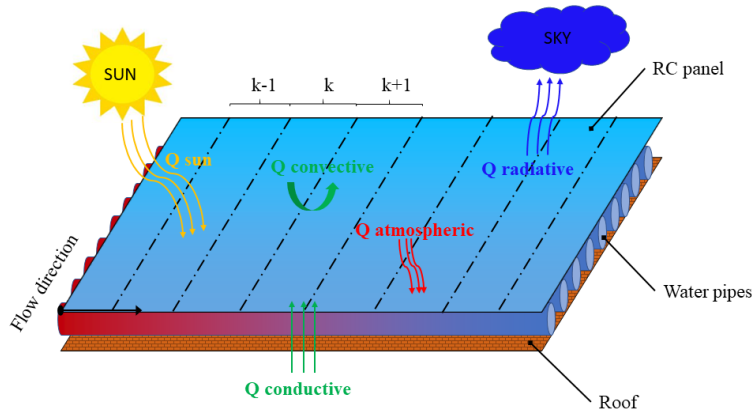


Figure 3. Schematic of the RC panel discretized into segments and different heat transfer processes.

B. PCM tanks model

The proposed storage system consists of two PCM storage tanks having two different melting temperatures. During the night, the PCM stores the cold energy from the water and solidifies, and this energy is released into the hot water during daytime

(see Figure 4). Each tank is modeled as a fully insulated horizontal tank filled with spherical capsules containing PCM. The thermal model describing the behavior of this component is based on the following assumptions: (1) The width of each tank is negligible compared to its length; (2) the temperature of the water flowing through the tank varies only in one direction: longitudinally along the flow direction; (3) the heat transfer in the volume of the sphere is neglected; (4) the temperature gradient of the PCM in the radial direction is negligible; (5) the material constituting the PCM capsuled shell has a negligible thermal resistance.

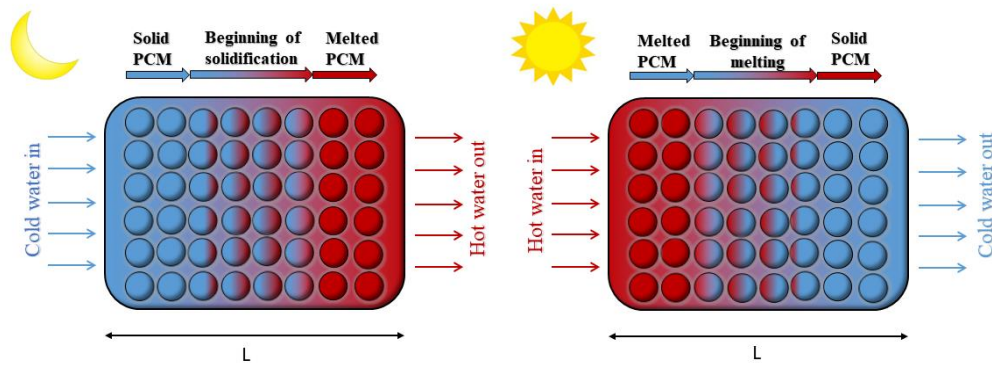


Figure 4. Schematic of one PCM tank during solidification (nighttime) and melting (daytime).

Each tank is divided into N segments along its length. Each segment has the same height equal to the diameter of the capsules and contains the same number of PCM. A simplified mathematical model is adopted to predict the temperature of the water and that of the PCM in each tank. The model is divided into two sub-models depending on the temperature of the PCM (T_{pcm}).

(1) Sub-model 1 is adopted when $T_{pcm} \neq T_{melting}$, and consists of solving the enthalpy change equation on each segment i of each storage tank. Based on assumption (5), the heat transfer between the water and the PCM capsules in each tank mainly happens through convection. The energy balance is shown in equation (3) where the index j represents the tank about which the energy equation is applied $m_{pcm,j}$ and $N_{pcm,j}$ are respectively the mass of each PCM sphere and the number of PCM in each segment of tank j .

$$m_{pcm,j} N_{pcm,j} C_{p,pcm,j} \frac{dT_{pcm,j}(i)}{dt} = (T_{w,tank,j}(t, i) - T_{pcm,j}(t, i)) h_{pcm,j} A_{pcm,j} \quad (3)$$

The left side of equation (3) represents the transient storage capacity of PCM in tank j which depends on the specific heat capacity of the PCM in tank j ($C_{p,pcm,j}$). The right side represents the convective heat flow between the PCM in tank j and the water, this heat transfer method is highly affected by $h_{pcm,j}$ – the heat transfer coefficient between the water and the PCM in tank j . $T_{w,tank,j}(t, i)$ and $T_{pcm,j}(t, i)$ are the temperatures of the water and the PCM in tank j at segment i and time t respectively, and $A_{pcm,j}$ is the total area of the PCM spheres in one segment of tank j .

(2) Sub model 2 is adopted when $T_{pcm} = T_{melting}$. At this point, the PCM undergoes a phase change process modeled by equation (4).

$$m_{pcm,j} L_{f,j} \frac{\partial f_{i,j}}{\partial t} = (T_{w,tank,j}(t, i) - T_{pcm,j}(t, i)) h_{pcm,j} A_{pcm,j} \quad (4)$$

Where $f_{i,j}$ and $L_{f,j}$ are the melted fraction and the latent heat of fusion of PCM in the segment i of tank j , respectively.

As for the water flowing in the PCM tanks, the global conservation of energy in each segment of each tank is given by equation (5). The left side of the equation

designates the energy stored in the water. The first term of the right side represents the heat exchange between the water and the spherical capsules while the second term represents the net convective heat flow.

$$\begin{aligned} \rho_w V_{w,segment,j} C_{p,w} \frac{dT_{w,tank,j}}{dt} & \quad (\\ & = \dot{m}_{w,tank} C_{p,w} (T_{w,tank,j}(t, i - 1) - T_{w,tank,j}(t, i)) \\ & - h_{pcm,j} A_{pcm,j} (T_{w,tank,j}(t, i) - T_{pcm,j}(t, i)) \end{aligned} \quad 5)$$

Where $V_{w,segment,j}$ and $\dot{m}_{w,tank}$ are the volume of water in one segment of tank j and the mass flow rate of water flowing through the tanks, respectively.

C. The Space Model

The cooling load of the considered residence is calculated by developing a space model using the transient simulation software TRNSYS [26]. Such software is known for its accurate estimation of building cooling load [27, 28]. The multi-zone building model type56 subroutine is employed to determine the cooling load in question. Furthermore, the energy rate mode is set with typical Kuwaiti indoor conditions: indoor air temperature of 23 °C and 50 % relative humidity [29]. The model takes as input the physical and thermal properties of the building envelope, the internal gains as well as the weather data.

CHAPTER IV

NUMERICAL METHODOLOGY

The operation of the integrated system is assessed by conducting numerical simulations following the chart presented in Figure 5. The space cooling load is first obtained for the entire Kuwaiti summer season using the simulation program TRNSYS [26]. This software requires detailed information regarding the geometrical and thermal properties of the considered residential house, as well as the outdoor and indoor set conditions. The multi-zone building model type56 thus estimates the hourly cooling load of the residential house, which is set as input to the developed mathematical model in MATLAB [30]. The latter further requires additional input like the weather data, RC panel properties and PCM tanks properties. The simplified transient model consists of an implicit first-order time integration scheme, to solve the energy balance of the RC panel and PCM tank models. Note that a time step of 100 s was adopted after conducting a time step independence test.

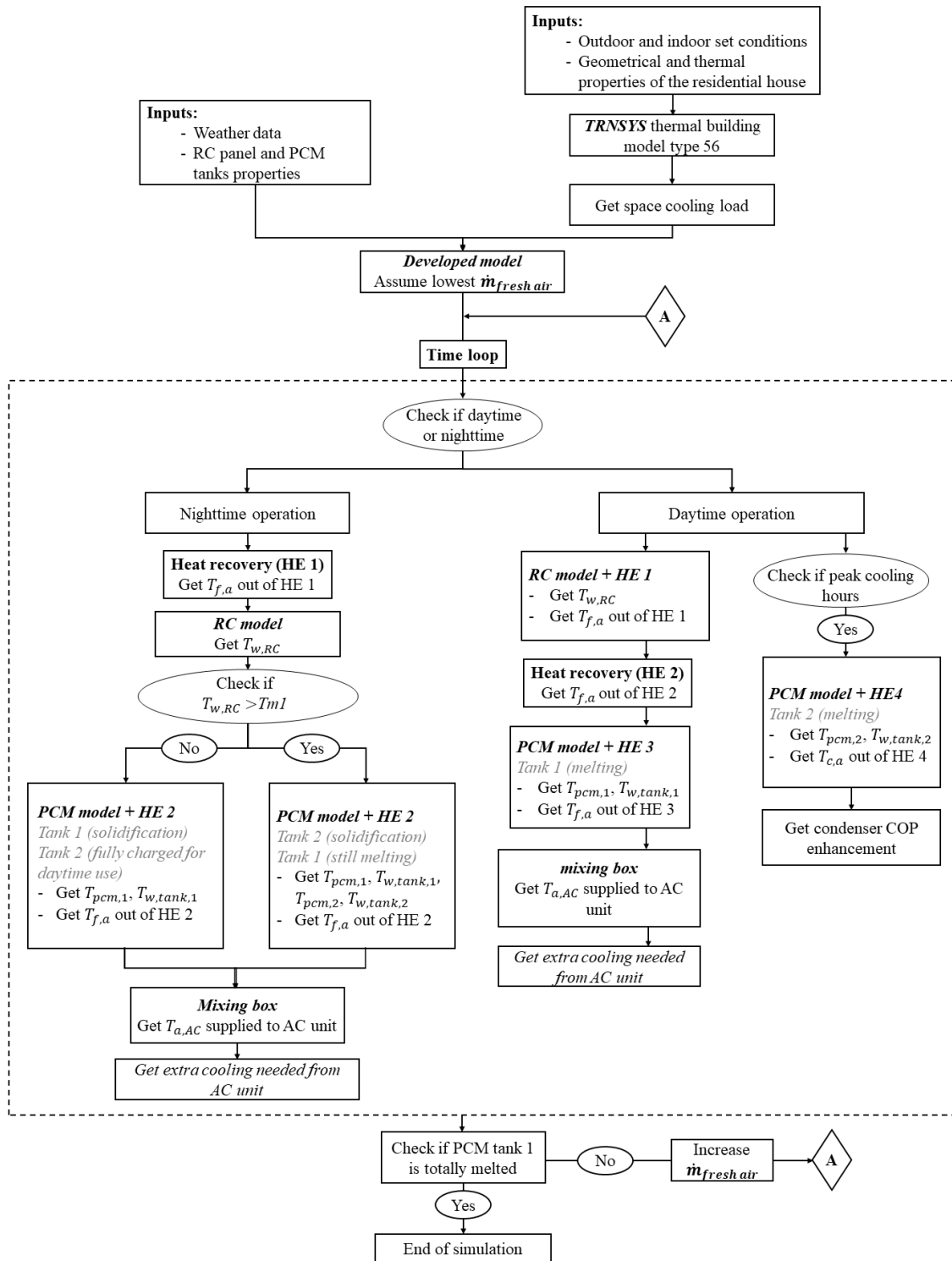


Figure 5. Flow chart of the numerical modeling methodology.

For each considered month, the initial fresh air flowrate ($\dot{m}_{fresh\ air}$) provided to the space is set to the minimum fresh air requirement recommended by ASHRAE (7.5 l/s/person) [31]. During each simulation, the following is conducted in the model: For nighttime operation, the fresh air is first cooled by heat recovery process in HE 1, and the resulting fresh air temperature $T_{f,a}$ is obtained. Then, the RC sub-model predicts the temperature of the water flowing through the panel ($T_{w,RC}$) by solving the corresponding differential equations iteratively. Based on $T_{w,RC}$, the solver checks whether the early or late night operation is needed to be simulated: if $T_{w,RC} > T_{m1}$, the early night operation is simulated as tank 2 is still charging while tank 1 is being used for air cooling; otherwise, tank 2 is completely solidified and tank 1 should start the charging process, and thus, the late night operation starts. Accordingly, for each operation, the temperature of the water ($T_{w,tank}$) and PCM spheres (T_{pcm}) in tanks 1 and 2 are calculated via the PCM tank models, along with the temperature of the fresh air ($T_{f,a}$) leaving the water-air heat exchanger HE 2. Then, mixing between the fresh and return air is simulated to obtain the total supply air temperature $T_{a,AC}$ supplied to the AC unit for further cooling to meet the required nighttime cooling load of the space. For daytime operation, the RC sub-model is also used to determine the water temperature variation throughout the panel ($T_{w,RC}$), and the resulting fresh air temperature $T_{f,a}$ exiting HE 1 is obtained. Further air-cooling occurs in HE 2 due to the heat recovery process. Then, the water exiting PCM tank 1 is used to additionally cool the air in HE 3. Thus, using the PCM tank model, $T_{w,tank,1}$ and $T_{pcm,1}$ are predicted for tank 1, along with the resulting $T_{f,a}$ out of HE 3. Then mixing of the fresh air with the return air is simulated to get the total supply air temperature $T_{a,AC}$ supplied to the AC

unit to reach eventually the required cooling load of the space. Note that during peak cooling hours of the day, the outdoor ambient air temperature (T_{amb}) is higher than the melting temperature of Tank 2 (T_{m2}), and the COP of the condenser is at its lowest, thus, PCM tank 2 is used to cool air entering the condenser ($T_{c,a}$). So $T_{w,tank,2}$ and $T_{pcm,2}$ are predicted via the PCM tank model, while $T_{c,a}$ resulting from the heat exchange with the water exiting tank 2 in HE 4 is obtained. Thus, the enhancement of the condenser COP is assessed for these specific peak hours.

To advance from one-time step to another in a simulation, a convergence criterion was set, where the difference between two consecutive iterations of any output parameter should be less than 10^{-5} . Note that simulations are repeated over a number of cycle days to reach a steady periodic solution. After reaching convergence, the solver checks the state of PCM tank 1: if this tank is totally melted at the end of the early night period, the simulation ends and the adopted $\dot{m}_{fresh\ air}$ is adequate; otherwise, $\dot{m}_{fresh\ air}$ is increased, and the simulation is repeated. Thus, the amount of fresh air increase provided by the proposed system operation is assessed.

CHAPTER V

CASE STUDY

In order to assess the performance of the proposed system, a typical Kuwaiti building is investigated for the entire cooling season: April through October. The weather data for each considered month is obtained from the Kuwait meteorological center [32]. Figure 6 shows the ambient temperature and solar radiation for the representative day of each summer month. Furthermore, the relative humidity ranged between 10 % and 60 % throughout the cooling season.

The considered building is a two-story residential house of height 13.65 m, each floor having a surface area of (25 m × 20 m). The considered residential villa is divided into four zones: the living room, the bedroom, the kitchen and the bathrooms. The physical composition of the space envelope is presented in Table 1. As for the windows, the glazing U-value is set to 3.33 w/m².K and SHGC is 0.36 [33]. The residential house is considered occupied by six people, each having a sensible load of 75 W and a latent load of 55 W. Other internal gains also account for the electric equipment and lights in the residence (refrigerator, water cooler, microwave oven etc.). As for the PCM storage tanks, they are fully insulated water/PCM tanks. The PCM is placed inside highly conductive spherical capsules. When the temperature of the water surrounding the PCM spheres is low, they solidify while releasing their energy to the water. Otherwise, the PCM spheres melt as they absorb heat from the surrounding water. The PCM melting temperature used in each tank should be set based on the available cooling power produced by the RC panel during the night-time period. Thus, this is chosen after conducting simulations and is presented in the system sizing section. Furthermore, the

material of the RC panel reported in the study of Hua et al. [20] is adopted in this work, due to its meaningful daytime radiative cooling, its scalable coating that has significant potential in large scale applications at a relatively low cost. It consisted of a double-layer nanoparticle-based coating structure. The double layer-coatings are on top of an aluminum substrate and are composed of a reflective layer on top of an emissive layer. The reflective material is chosen to be a common material with stable chemical properties and high refractive index: titanium dioxide (TiO_2), with a thickness of 25 μm . The latter is highly reflective in the solar spectrum and transparent in the mid infrared spectrum. Silicon dioxide (SiO_2) is chosen to achieve selective emission in the “transparency window” with a thickness of 20 μm .

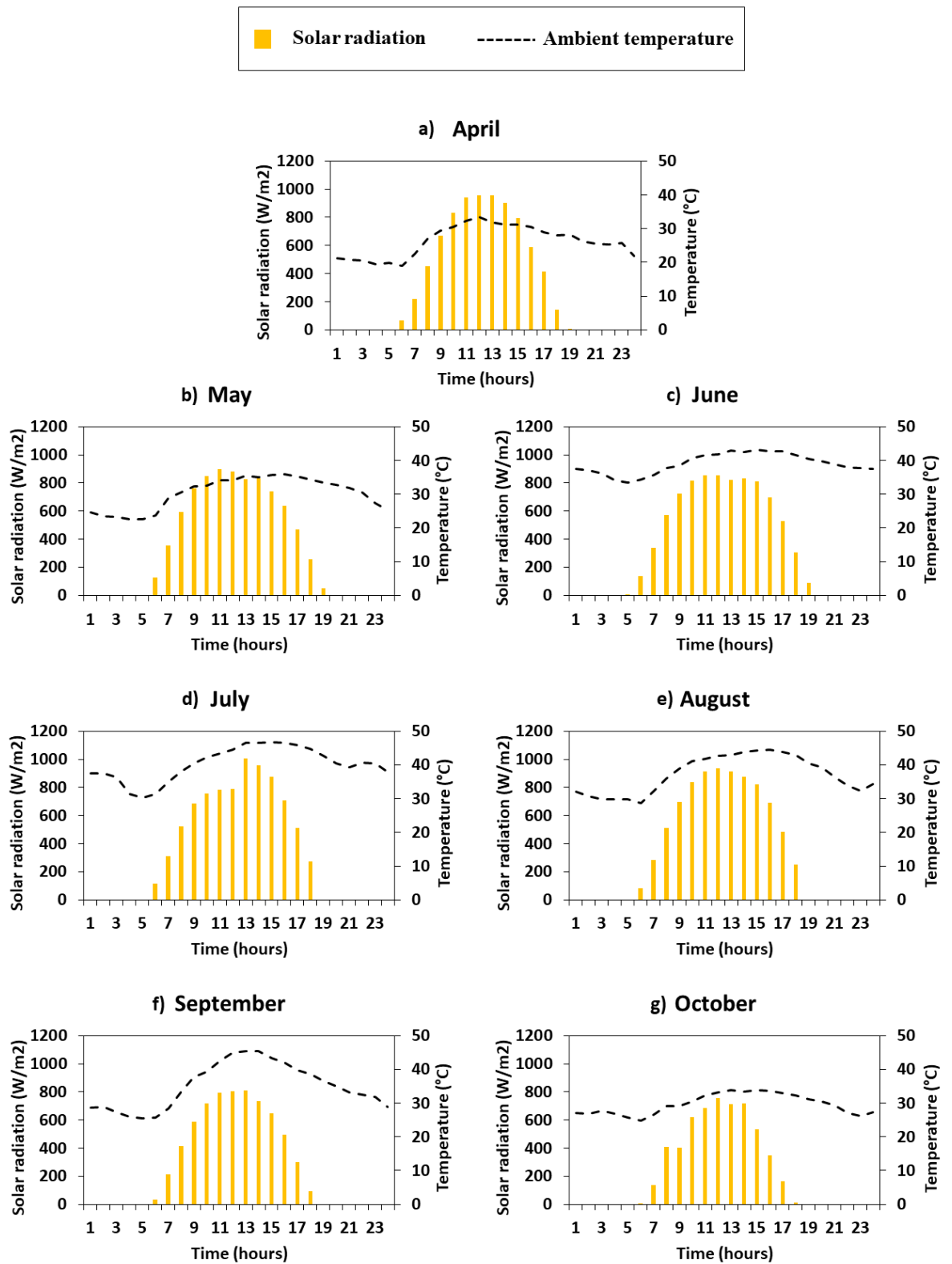


Figure 6. Hourly variation of temperature and solar radiation for a representative day of each cooling month.

Table 1. Thermal details of the envelope layers (Inside to Outside).

Layer	Thickness (mm)	Density (kg/m ³)	<i>C_p</i> (kJ/kg·K)	RSI-Value (m ² -K/W)
Inside surface resistance	-	-	-	0.1206
102mm LW concrete block	102	608.7	0.837	0.2668
RSI-1.2 board insulation	25.4	32.04	0.921	1.2229
203mm common brick	203	1922.22	0.837	0.2795
203mm HW concrete	203	2242.58	0.837	0.1174
Outside surface resistance	-	-	-	0.0586

CHAPTER VI

RESULTS

In this section, the integrated model validation of the hybrid RC-PCM and AC system is presented followed by the results of the system sizing for the case study of the typical Kuwaiti residence. The system operation is analysed over the entire cooling months to present the increase in fresh air supply over the conventional system as well as the energy savings associated with the system implementation.

A. Model validation

The developed model in this work is an integration of previously validated and well-documented models in literature [20, 34]. For the RC panel model, the model of Katramiz et al. [22] was based on the experimentally validated model of Hua et al. [20]: by conducting experimental measures in the moist weather of Shanghai, they reported a 5 °C panel temperature below ambient at night, in the range of the theoretical results of 4 – 6 °C below ambient obtained during high humidity night conditions. After taking the same geometric and climatic conditions as in the study of Hua et al. [20], a maximum discrepancy of 5.8% was found between the results reported by Hua et al. [20] and those obtained from the developed model of Katramiz et al. [28]. As for the water/PCM tank model, it consisted of the spherical capsules PCM tank model of Ismail et al. [34] that was validated by comparison with experimental tests. They reported that the experimental and numerical findings were in good agreement: a maximum error of 7.2 % was reported between the experimental and numerical data.

B. System sizing

To ensure the successful operation of the proposed system, it is crucial to properly size its different components. For the RC panel sizing, it is well established that the increase in the area of the panel increases its cooling capacity. Thus, in this work, a maximum RC panel area was set to cover 70% of the roof. Note that the remaining area is dedicated for other system components as storage tanks. The resulting water temperature leaving the RC panel $T_{w,RC}$ during nighttime period varied between 29 °C during early night hours and around 16 °C at the end of the night period.

Subsequently, the melting temperatures of the PCM tanks were fixed according to

$T_{w,RC}$:

- Since PCM tank 1 is used to further cool the fresh air that has already harvested the cooling power of the exhaust air by heat recovery, the melting temperature of the PCM in tank 1 must be lower than that of the exhaust air (i.e. lower than around 24 °C). Thus, T_{m1} must be between 24 °C and 16 °C (lowest $T_{w,RC}$). RT22HC paraffin was therefore chosen for tank 1 as the low melting temperature PCM, with T_{m1} of 22 °C.
- On the other hand, the melting temperature of PCM tank 2 should be selected based on $T_{w,RC}$ during the early night hours. As a result, RT28HC paraffin was used in storage tank 2, with a high melting temperature T_{m2} of 28 °C.

These PCMs are commercially available by Rubitherm [35]. As for the PCM storage tanks, they were sized to be able to harvest all the cooling power produced by the RC panel during nighttime. Since the performance of the RC panel is highly affected by the outdoor conditions (ambient temperature, relative humidity, solar radiation etc.),

the sizing of the system should be designed according to the peak summer month. Thus, the cooling loads for each month were obtained using TRNSYS, and benchmarked with reported cooling load data in literature for Kuwaiti residences [36]. As a result, July was found to be the month with the peak cooling loads, ranging between a minimum of 17 W/m² during nighttime and a maximum of 38 W/m² during daytime. Accordingly, the sizing of each PCM storage tank was based on the weather data of July. The mass flow rate of the air supplied to the space was fixed to 5 kg/s [28]. After running many simulations to obtain the lowest water temperature at the exit of the RC panel during the month of July, the mass flow rate of water flowing in the RC loop was set to 0.18 kg/s. During July, the PCM spheres in tank 1 started solidifying at late hours of the night (around 1:00 A.M) when the temperature of the water out of the panels was lower than T_{m1} (22 °C). Thus, the needed PCM mass in tank 1 was fixed based on the cooling power of the RC panel from 1:00 A.M until the end of the nighttime period (around 6:00 A.M). As for the PCM spheres in tank 2, they should undergo solidification during early nighttime hours (around 7:00 P.M) when the temperature of the water exiting the RC panel is lower than T_{m2} (28 °C). Note that the size of tank 2 was fixed based on the cooling load provided by the RC panel during early nighttime period, i.e. before the temperature of the water exiting the RC panel was lower than T_{m1} . Accordingly, the PCM storage tanks were adequately sized: each tank is totally melted at the end of its corresponding operation schedule, with the PCM spheres reaching their melting temperature (T_{m1} and T_{m2} respectively). This sizing strategy ensures that the RC power is only used to solidify the PCM storage tanks. The operational parameters as well as the thermos-physical properties of each PCM are shown in Table 2.

Table 2. Characteristics of the PCM storage tanks.

	Tank 1	Tank 2
Name of Material	RT22HC Paraffin	RT28HC paraffin
PCM melting temperature [°C]	22	28
Latent heat of fusion L_f [kJ/kg]	250	190
Specific heat capacity C_{pcm} [kJ/kg·K]	2	2
Density [kg/m ³]	800	750
Total mass [kg]	160	200
Width [m]	0.45	0.50
Length [m]	2	2
High [m]	0.45	0.5

C. System operation

After sizing the system, its operation was assessed for the entire cooling season by conducting simulations using the developed model. The nocturnal cooling power of the RC panel was harvested by the PCM tanks. This stored cooling power was used to offset the increase in energy consumption associated with conditioning the high temperature fresh air intake. Furthermore, the performance of the system was enhanced due to the improvement of the COP of the AC system and reduction in the required overall cooling load with respect to the conventional AC system operation.

As previously mentioned, PCM tank 1 was integrated with the RC panel to pre-cool the fresh air. This provided the opportunity to increase the amount of fresh air supplied to the space, with zero energy consumption compared to the conventional AC system. Figure 7 presents the fresh air flowrate per person ($\dot{m}_{fresh\ air}$) supplied to the space, which exceeded the minimum requirements of 7.5 l/s/person [31] for all the summer months. Note that for each considered summer month, $\dot{m}_{fresh\ air}$ was maintained constant throughout the day, and that the entire ventilation load was met by

the proposed passive system. The smallest amount of fresh air supplied to the space (30 l/s/person) was observed for the peak month of the cooling season (i.e. July): four times higher than the minimum required amount. This portion of fresh air increased for the moderate months until reaching 190 l/s/person, exceeding the minimum required amount by twenty-five times for the month of April. This was predictable due to the relatively low outdoor conditions during this month (Figure 6.a).

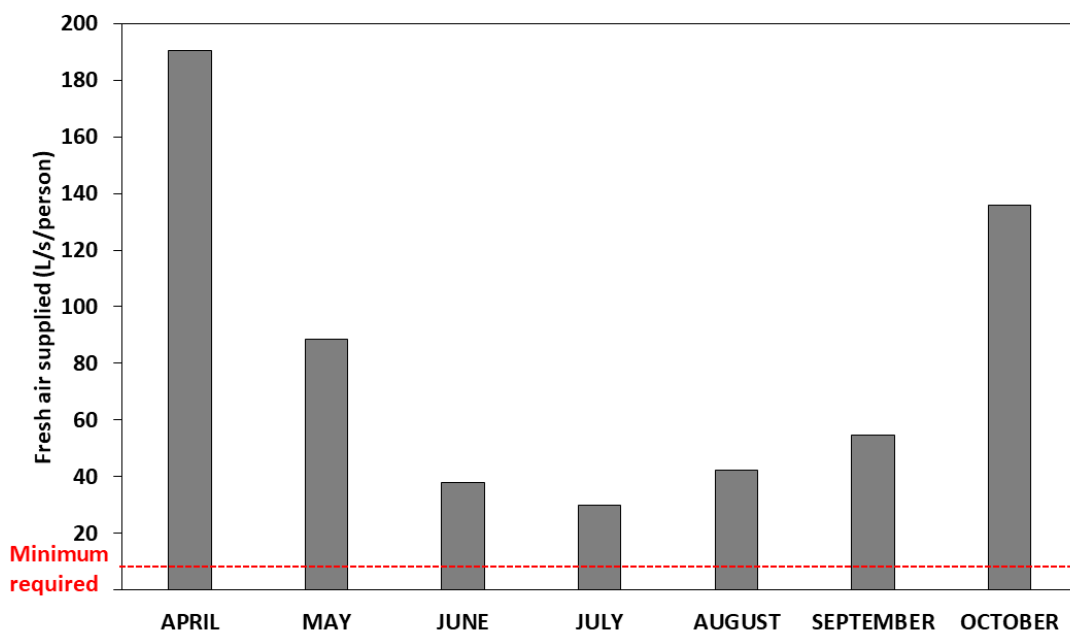


Figure 7. Flow rate of fresh air supplied to the space for the entire cooling season.

As previously mentioned, the proposed system was able to meet the entire ventilation load for all the considered months based on the corresponding $\dot{m}_{fresh\ air}$ (Figure 7). The average ventilation savings ($Q_{ventilation\ savings}$) of the proposed system with respect to the conventional AC system with heat recovery, for the same fresh air intake is presented in Figure 8. In order to get the same IAQ relying only on the conventional AC system, an average ventilation load of 0.95 kW will be required

per day for the entire cooling season. This required load was completely met by the proposed system. Furthermore, for the off-peak months, the system was capable of reducing the fresh air temperature to the AC below that of the return air (T_{return}). This reduction was mostly observed when the RC cooling power was high enough, especially in moderate climate conditions. The resultant mixture of return and fresh air (\dot{m}_{supply}) was thus at a temperature $T_{a,AC}$ less than T_{return} . Additional savings in the AC system cooling load were consequently achieved. These savings were calculated using equation (6):

$$Q_{additional\ saving} = \dot{m}_{supply} C_{p,a} (T_{return} - T_{a,AC}) \quad (6)$$

Figure 9 shows the average additional cooling load savings for a representative day of each considered summer month. As predicted, for the peak month of July, the system was only capable of meeting the ventilation load, and no additional savings were reported. Whereas, for the remaining months, the system was able to provide considerable additional savings for the cooling load, with a maximum of 4.1 kW for the month of April. Note that the trend of variation of $Q_{ventilation\ savings}$ and $Q_{additional\ savings}$ between the summer months followed that of fresh air intake (Figure 7). An average of 2 kW additional cooling load savings was therefore achieved daily during the entire Kuwaiti summer season.

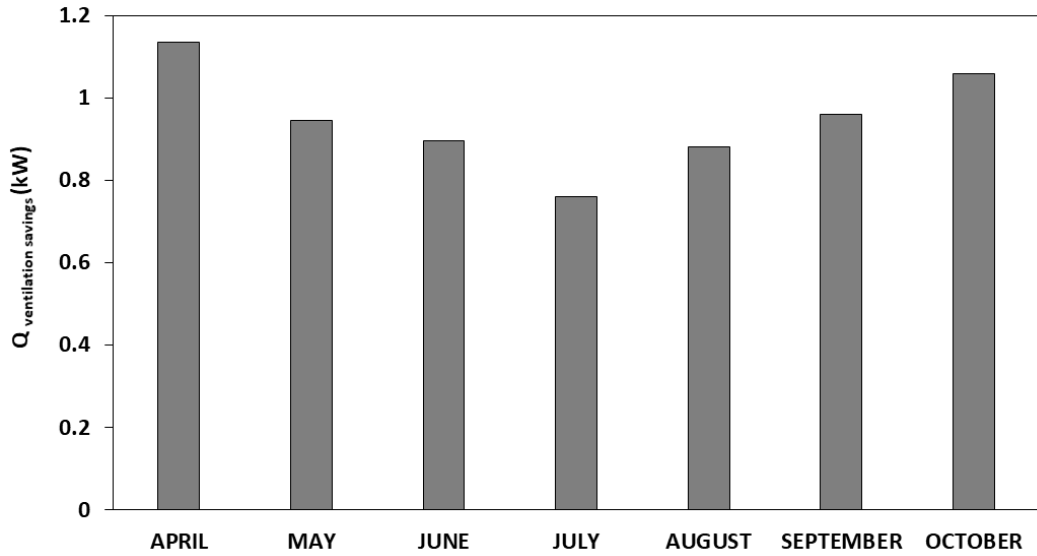


Figure 8. Average ventilation savings for a representative day of the cooling season.

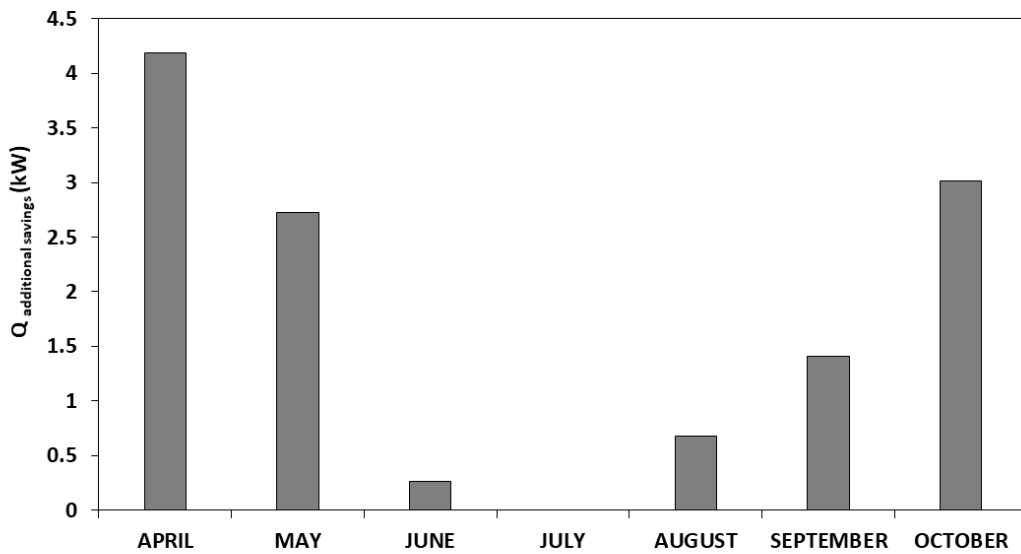


Figure 9. Average additional savings in the cooling load for a representative day of the cooling season.

The use of tank 1 was able to enhance the performance of the AC system by meeting the ventilation load and procuring additional cooling load savings. Further enhancement can be achieved by using the cold power stored in PCM tank 2 to cool the

ambient air entering the condenser of the AC unit during the peak daytime hours. In fact, the ambient air temperature highly affects the COP of an air-cooled condenser [37]. Figure 10 shows the hourly schedule of the PCM tank 2 operation and corresponding COP enhancement percentage for each considered summer month. The operation schedule of tank 2 varied from month to another, as it depends on two parameters: the peak hours period during which the COP was at its lowest, as well as the difference between the ambient temperature (T_{amb}) and the melting temperature of tank 2 (T_{m2}). As expected, the maximum COP enhancement was achieved during the peak month of July: T_{amb} was largely exceeding T_{m2} (28 °C), which induced a 14.3 % COP enhancement for a period of around 3 hours (between 13:00 P.M and 16:00 P.M), until the total melting of tank 2. This percentage decreased for the moderate months, where T_{amb} was closer to T_{m2} . Thus, the lowest COP enhancement was obtained for the month of October (5 %), however with a long operation period of around 6 hours until the depletion of the cooling power of PCM tank 2 (i.e. total melting of the PCM).

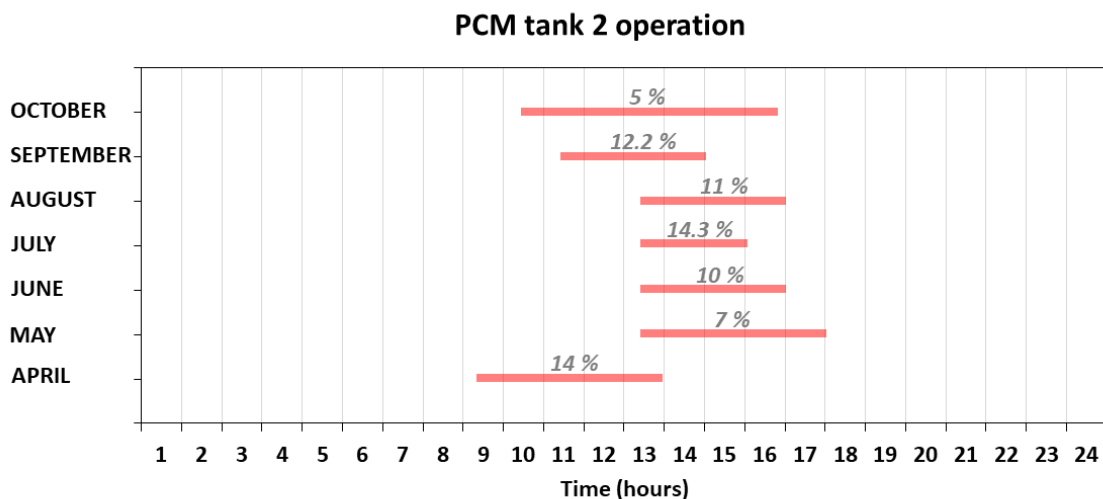


Figure 10. Hourly schedule of the PCM tank 2 operation and corresponding percentage of COP enhancement for each considered summer month.

D. Energy saving analysis

In this study, the performance of the AC system was enhanced due to the implementation of the proposed system. The usage of tank 1 helped in reducing the total cooling load q_L of the villa: the entire ventilation load was met compared to the conventional AC system and additional savings were achieved during off-peak months (Figure 9). On the other hand, tank 2 was able to enhance the COP by cooling the ambient air entering the condenser. The combination of those two operations resulted in a remarkable decrease in the total energy consumption of the AC system which was assessed by the following equation:

$$E = \frac{q_L}{COP} \quad (6)$$

Where E and q_L are the total energy consumption of the AC system and the cooling load of the villa, respectively. Figure 11 shows the percentage of the total energy consumption reduction for the Kuwaiti entire cooling season in comparison to the case when the same $\dot{m}_{fresh\ air}$ was treated by the conventional AC system. An average of 22.2 % reduction in energy consumption was found for the entire considered cooling season, with a maximum of 39 % in April due to its moderate weather conditions that improved the performance of the RC panel and led to an enhancement in the overall system effectiveness. However, a minimum of 6.7 % was observed for the peak summer month of July where the outdoor conditions were extremely high.

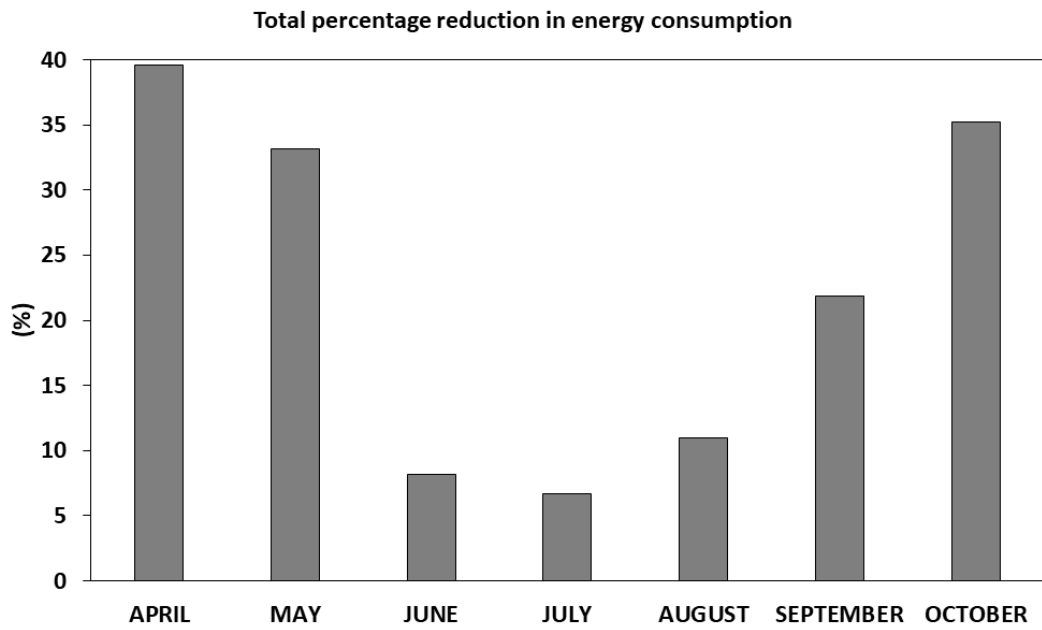


Figure 11. Average percentage reduction of the energy consumption using the proposed system with respect to the conventional mechanical cooling system for the entire summer season.

CHAPTER VIII

CONCLUSION

This work evaluated the integration of a passive system composed of an RC panel combined with two PCM storage tanks (tank 1 and tank 2). The cooling power of the RC panel was stored during nighttime in the storage tanks. Tank 1 was used for cooling the supplied fresh air and tank 2 was implemented to enhance the AC system COP. A set of simulations was conducted for a typical Kuwaiti residential building for the entire cooling period which extends from April to October. It was found that using tank 1 resulted in an increase in the fresh air intake at zero energy cost, while minimizing the intervention of the mechanical cooling system. Furthermore, the implementation of tank 2 led to an increase of the COP by an average of 10.5 %. The proposed system was hence able to decrease the overall energy consumption by 22.2 % with respect to the conventional AC system providing the same IAQ. This highlights the beneficial role of integrating the proposed passive system to assist the AC system in offsetting the increase in energy consumption related to the conditioning of the high temperature fresh air intake and providing high IAQ levels in the hot climate of Kuwait.

REFERENCES

1. Alotaibi, S., *Energy consumption in Kuwait: Prospects and future approaches*. Energy Policy, 2011. **39**(2): p. 637-643.
2. Li, Y., et al., *Role of ventilation in airborne transmission of infectious agents in the built environment-a multidisciplinary systematic review*. Indoor air, 2007. **17**(1): p. 2-18.
3. Dai, H. and B. Zhao. *Association of the infection probability of COVID-19 with ventilation rates in confined spaces*. in *Building Simulation*. 2020. Springer.
4. Park, J., T. Kim, and C.-s. Lee, *Development of thermal comfort-based controller and potential reduction of the cooling energy consumption of a residential building in Kuwait*. Energies, 2019. **12**(17): p. 3348.
5. Kellow, M., *Kuwait's approach to mandatory energy-conservation standards for buildings*. Energy, 1989. **14**(8): p. 491-502.
6. Williams, D., et al., *Climate change influence on building lifecycle greenhouse gas emissions: Case study of a UK mixed-use development*. Energy and Buildings, 2012. **48**: p. 112-126.
7. Zinzi, M. and G. Fasano, *Properties and performance of advanced reflective paints to reduce the cooling loads in buildings and mitigate the heat island effect in urban areas*. International Journal of Sustainable Energy, 2009. **28**(1-3): p. 123-139.
8. Al Touma, A., et al., *Solar chimney integrated with passive evaporative cooler applied on glazing surfaces*. Energy, 2016. **115**: p. 169-179.
9. Baakeem, S.S., et al., *The possibility of using a novel dew point air cooling system (M-Cycle) for A/C application in Arab Gulf Countries*. Building and Environment, 2019. **148**: p. 185-197.
10. Harrouz, J.P., K. Ghali, and N. Ghaddar, *Integrated solar-Windcatcher with dew-point indirect evaporative cooler for classrooms*. Applied Thermal Engineering, 2021. **188**: p. 116654.
11. Head, A.K., *Method and means for producing refrigeration by selective radiation*. 1962, Google Patents.
12. Gentle, A.R. and G.B. Smith, *Radiative heat pumping from the earth using surface phonon resonant nanoparticles*. Nano letters, 2010. **10**(2): p. 373-379.
13. Orel, B., M.K. Gunde, and A. Krainer, *Radiative cooling efficiency of white pigmented paints*. Solar energy, 1993. **50**(6): p. 477-482.
14. Yu, N., et al., *Systems and methods for radiative cooling and heating*. 2019, Brookhaven National Lab.(BNL), Upton, NY (United States).
15. Jeong SY, T.C., Wong YM, Chao CY *Passive radiative cooler based on biomimetic metasurface from Saharan silver ants*. in *Proceedings of the 4th International Conference on Building Energy and Environment*. 2018. Melbourne, Australia.

16. Hu, M., et al., *Implementation of Passive Radiative Cooling Technology in Buildings: A Review*. Buildings, 2020. **10**(12): p. 215.
17. Ahmad, M.I., H. Jarimi, and S. Riffat, *Nocturnal cooling technology for building applications*. 2019: Springer.
18. Jeong, S.Y., et al. *A numerical study of daytime passive radiative coolers for space cooling in buildings*. in *Building Simulation*. 2018. Springer.
19. Zhao, B., et al., *Radiative cooling: A review of fundamentals, materials, applications, and prospects*. Applied Energy, 2019. **236**: p. 489-513.
20. Bao, H., et al., *Double-layer nanoparticle-based coatings for efficient terrestrial radiative cooling*. Solar Energy Materials and Solar Cells, 2017. **168**: p. 78-84.
21. Zhang, S. and J. Niu, *Cooling performance of nocturnal radiative cooling combined with microencapsulated phase change material (MPCM) slurry storage*. Energy and Buildings, 2012. **54**: p. 122-130.
22. Katramiz, E., N. Ghaddar, and K. Ghali, *Daytime radiative cooling: To what extent it enhances office cooling system performance in comparison to night cooling in semi-arid climate?* Journal of Building Engineering, 2020. **28**: p. 101020.
23. Kauranen, P., K. Peippo, and P. Lund, *An organic PCM storage system with adjustable melting temperature*. Solar Energy, 1991. **46**(5): p. 275-278.
24. Stritih, U. and V. Butala, *Energy saving in building with PCM cold storage*. International journal of energy research, 2007. **31**(15): p. 1532-1544.
25. Mihalakakou, G., A. Ferrante, and J. Lewis, *The cooling potential of a metallic nocturnal radiator*. Energy and Buildings, 1998. **28**(3): p. 251-256.
26. TRNSYS. *Thermal energy system specialists*. Available from: <http://www.trnsys.com/>.
27. Pagliarini, G., C. Corradi, and S. Rainieri, *Hospital CHCP system optimization assisted by TRNSYS building energy simulation tool*. Applied Thermal Engineering, 2012. **44**: p. 150-158.
28. Katramiz, E., et al., *Sustainable cooling system for Kuwait hot climate combining diurnal radiative cooling and indirect evaporative cooling system*. Energy, 2020. **213**: p. 119045.
29. Al-Rashidi, K., D. Loveday, and N. Al-Mutawa, *Impact of ventilation modes on carbon dioxide concentration levels in Kuwait classrooms*. Energy and Buildings, 2012. **47**: p. 540-549.
30. MATLAB. Available from: <https://www.mathworks.com/products/matlab.html>.
31. ASHRAE STANDARD 62-2001 *Ventilation for acceptable indoor air quality*. 2001; Available from: https://www.ashrae.org/File%20Library/Technical%20Resources/Standards%20and%20Guidelines/Standards%20Addenda/62-2001/62-2001_Addendum-n.pdf.
32. Aviation-Kuwait, D.G.o.C. *Meteorological Department*. Available from: <https://www.met.gov.kw/>.

33. *Ministry of Electricity and Water MEW /R-6/2016 code of practice*. Available from: https://kupdf.net/download/mew-r6-2016_59d22da308bbc57429686f94_pdf.
34. Ismail, K. and J. Henriquez, *Numerical and experimental study of spherical capsules packed bed latent heat storage system*. *Applied Thermal Engineering*, 2002. **22**(15): p. 1705-1716.
35. Rubitherm. *Rubitherm, Phase Change Material*. Available from: <https://www.rubitherm.eu/en/index.php/productcategory/organische-pcm-rt>.
36. Al-Ajmi, F.F. and V. Hanby, *Simulation of energy consumption for Kuwaiti domestic buildings*. *Energy and buildings*, 2008. **40**(6): p. 1101-1109.
37. Hajidavalloo, E. and H. Eghtedari, *Performance improvement of air-cooled refrigeration system by using evaporatively cooled air condenser*. *International journal of refrigeration*, 2010. **33**(5): p. 982-988.